American Mineralogist, Volume 87, pages 205–216, 2002

Characterization of coexisting NH_4- and K-micas in very low-grade metapelites

FERNANDO NIETO

Instituto Andaluz de Ciencias de la Tierra, Universidad de Granada-C.S.I.C., Avenue Fuentenueva, 18002 Granada, Spain

ABSTRACT

Organic-rich Carboniferous shales with associated coal seams, from the *Bacia Carbonífera do Douro-Beira* (north Portugal)**,** have been studied by TEM as well as by a variety of other methods. NH_4 and K micas and berthierine form small subparallel packets of a few layers separated by low-angle boundaries. One- and two-layer ordered polytypes, with some spot enlargement typical of minor disorder, occur in the NH_4 micas (i.e., metamorphism tobelites). They exhibit all the characteristics commonly described for sub-greenschist-facies, including a lack of textural and chemical equilibrium. The compositions of the 2:1 layers vary considerably for both K- and NH_4-micas, and except for Ti, exhibit similar compositional ranges. The most significant compositional variations are explained by phengitic substitution (Si from 3 to 3.25, Fe + Mg from 0.1 to 0.3), but no evidence of an illitic substitution has been found. NH_4 in tobelites was determined by analysis of NH_3 using Nessler's reagent, basal spacing, and 1–(K + Na). The resulting values indicate NH_4 contents ranging from 30 to 59% of the interlayer site occupancy. At very low temperatures of metamorphism (e.g., North Sea), the intergrowths of NH_4 and K in micas is on the nanometer-scale. With an increase in temperature (e.g., Pennsylvania), NH_4- and K-micas are present as different minerals. The Douro-Beira samples represent a still higher-temperature case and, therefore, NH_4 and K can be present in the same interlayer sheet but with one cation being dominant. NH_4- and K-dominated micas have segregated into well-separated packets with scarce intergrowths and almost no mixed-layers. Hence they show a solvus relationship.

INTRODUCTION

The most common interlayer cation in low-grade metapelite micas is K. If the rock contains enough Al, Na micas may also be present; there may be a miscibility gap between the K-rich and Na-rich micas and the possible presence of micas with intermediate compositions. These intermediate phases have been described as illite-paragonite mixed-layers (Frey 1987), metastable intermediate NaK-mica (Jiang and Peacor 1993) or nanometer-scale mixtures of muscovite and bramalite (Livi et al. 1997). In addition, the presence of NH_4 represents a third important interlayer component (Guidotti and Sassi 1998a) that has not been studied thoroughly. This has been due, in part, to the intrinsic difficulty of analyzing NH_4 by in situ methods and, in part, to the typical defective character and small grain size of minerals in very low-grade metamorphic rocks, as most natural tobelites have been described in sub-greenschist-facies rocks (see below). In the present study, transmission electron microscopy (TEM) and analytical electron microscopy (AEM) have been employed to overcome this last limitation. Dioctahedral NH_4-dominant mica was discovered in nature and termed tobelite by Higashi (1982).

Synthetic examples

NH_4 micas were first described as synthetic products by Barrer and Dicks (1966), Eugster and Muñoz (1966), and Shigorova et al. (1981). NH_4 illite was produced as the final product of a series of experiments involving NH_4-bearing phyllosilicates (Hashizume et al. 1995). Intermediate products contained mixtures of randomly and ordered mixed layers of NH_4- and Na-montmorillonite and NH_4-illite. Sucha et al. (1998) found that the nature of the products obtained during hydrothermal synthesis of NH_4-illite strongly depends on the starting material. Tobelite with equimolar contents of K and NH_4 was obtained from synthetic gel at 300 °C.

Natural occurrences

Duit et al. (1986) determined the NH_4 content in metapelite micas and found a maximum of 1500 ppm for trioctahedral and 500 ppm for dioctahedral micas, the amount progressively diminishing with an increase in metamorphic grade. Similar concentrations were determined by Boyd (1997) by capacitance manometry. Cooper and Abedin (1981) found that the amount of fixed NH_4 in Gulf Coast shales in some cases constituted 7% of the fixed interlayer cations. Cuadros and Altaner (1998) showed that the bentonite illite-smectite samples contained considerable amounts of NH_4, averaging between 9 and 22% of the total fixed-cation content.

Juster et al. (1987) described NH_4-illites in mudrocks asso-

* E-mail: fnieto@ugr.es

ciated with the semi-anthracite and anthracite coal measures of Pennsylvania and interpreted NH_4-illites as forming from the replacement of K in illite by NH_3 expelled from coal seams during a very low-grade metamorphic coalification process. Likewise, Williams et al. (1989, 1992) concluded that NH_4 released from organic matter migrated with oil to become incorporated into phyllosilicates, with a maximum fixation coincident with the "oil window" (Williams and Ferrell 1991; Schroeder and McLain 1998). Daniels and Altaner (1990) interpreted the origin of the Pennsylvania tobelites in the same way as Juster et al. (1987), but considered kaolinite instead of K-illite as the precursor. The same type of origin was described by Liu et al. (1996) for NH_4-illites in coal-bearing strata in North China. Sucha et al. (1994) found NH_4-rich illite, together with K- and Na-illite, in shales associated with meta-anthracite coalfields in the Western Carpathians. The estimated formation temperature interval was 200–270 °C, as determined from vitrinite reflectance. Ward and Christie (1994) found NH_4-illite in the semi-anthracite material of Coal Seams in the Bowen Basin (Australia). In contrast, the mixed-layer, smectite-NH_4-illite described by Bobos and Ghergary (1999) in the fossil hydrothermal system of Harghita Băi (Romania) are not associated with coal or organic matter.

Wilson et al. (1992) described tobelites and NH_4-illites in veins of black shales from the Oquirrh Mountains, Utah and analyzed them by EMP methods. They reported a complete set of compositions, including O and N, with low to high NH_4 contents.

Identification

Juster et al. (1987) proposed the following criteria for the identification of tobelite: (1) large (≈10.15 Å) basal spacing; (2) characteristic relationships of intensities (I_{001}:I_{002}:I_{003} ratios of approximately 4:1:1 as compared to muscovite with ratios of approximately 4:1:3); (3) characteristic infrared absorption bands at 1430 cm^{-1} and in the range 3000–3400 cm^{-1}; and (4) the release of NH_3 gas in decomposition experiments. In as much as such criteria are not part of routine analyses, NH_4 illites might easily be overlooked. Drits et al. (1997) gave equations for determining the amount of NH_4 cations and the proportions of tobelite interlayers from d_{005}, which produced results that correlated well with those obtained by the isotope-dilution method (Lindgreen 1994). The NH_4 content has also been determined from the position of the (005) peak in powder X-ray diffraction (XRD) patterns or d_{005} by Juster et al. (1987), Sucha et al. (1994), and Higashi (2000).

MATERIALS AND METHODS

The *Bacia Carbonífera do Douro-Beira*, in the North of Portugal, is a narrow outcrop of continental Carboniferous rocks in the Central-Iberian Zone of the Iberian Variscan Belt that extends for 90 km from Porto in the NW to Viseu in the SE (Fig. 1). It includes polymict conglomerates, graywackes, and shales of Stephanian C age. Fossil plants and coal seams, worked in various mining districts, are very common. The coalification that led to the *Douro-Beira* peranthracites occurred between the 3rd and 4th Hercynian orogenic phases (late Carboniferous to early Permian). According to the coal rank, the temperature causing the coalification can be calculated at 270–360 °C (Lemos de Sousa 1978).

XRD studies reveal that the shales are composed of mica + quartz ± chlorite ± berthierine ± paragonite ± pyrophyllite ± feldspars. Berthierine is a phyllosilicate with trioctahedral-chlorite composition but a serpentine-like structure. The shales show illite crystallinity (IC) indices corresponding to anchizone and **b** mica parameters close to the limit between low and intermediate pressures, according to the Sassi and Scolary (1974) scale. The basal spacings of micas range from 9.95 to 10.18 Å. Those with the highest values of d_{001} displayed basal intensity ratios equivalent to those described by Juster et al. (1987) for NH_4-illites. In accordance with these data, samples Ge-6, Ge-7, and Ge-8 from the Germunde mine (Fig. 1), were selected for more detailed study. They are black shales with abundant organic matter and well-developed foliation. Optical study of thin sections reveals an abundant indistinguishable black matrix with very scarce detrital grains.

XRD studies were carried out using a Philips PW 1710 Powder Diffractometer with Cu$K\alpha$ radiation, graphite monochromator, and automatic divergence slit on randomly oriented powder mounts and separated fractions. The 2–20 μm fraction was separated by sedimentation through a column of water and the <2 μm fraction was separated by centrifugation. Oriented aggregates were prepared by sedimentation on glass slides. Preparation of samples and experimental conditions for IC measurements were carried out according to IGCP 294 IC Working Group recommendations (Kisch 1991). Our IC measurements (y) were transformed into Crystallinity Index Standard (C.I.S.) values (x) by means of the equation $y = 0.674x + 0.052$ ($r = 0.999$), obtained in our laboratory using the international standards of Warr and Rice (1994). The **b** parameters of mica were determined from the (060) peak measured on slices of rock cut normal to the sample foliation (Sassi and Scolary 1974). For all the spacing measurements, quartz from the sample itself was taken as an internal standard. We used the MAX routine for the Phillips PW 1710 Diffractometer, which locates the maximum of a peak by measuring the intensities at regular intervals. The experimental conditions of the final measurement were: distance between points of measurement = 0.005° 2θ; measurement time at each point = 1 s. The d_{001} spacing was obtained on oriented aggregate samples from the fifth mica peak. The <2 μm fraction was saturated with ethylene glycol for 24 h at a temperature of 60 °C and with dimethyl sulfoxide for 48 h at 80 °C, and heated at 550 °C for 2 h.

To study the effect of possible changes in the interlayer cations on XRD and IR spectra, a portion of the <2 μm fraction was saturated with Mg. For comparison, a smectite sample (Cuadros and Linares 1996) from La Serrata de Nijar in the Cabo de Gata volcanic area (Almeria Province, Spain) was saturated with NH_4 and studied by XRD and infrared methods (IR).

The IR spectra were recorded with a Nicolet 20SXB FT-IR spectrometer at the Centro de Instrumentación Científica (C.I.C.) at the University of Granada over the range 4000–400 cm^{-1} using wafers with 2.0 mg of the <2 μm fraction and 200 mg of KBr. Thermogravimetric analyses (TG) were carried out with 16 mg of <2 μm fraction in a SHIMADZU TGA-50H, at the C.I.C., in air at a heating rate of 10 °C/min. The qualitative

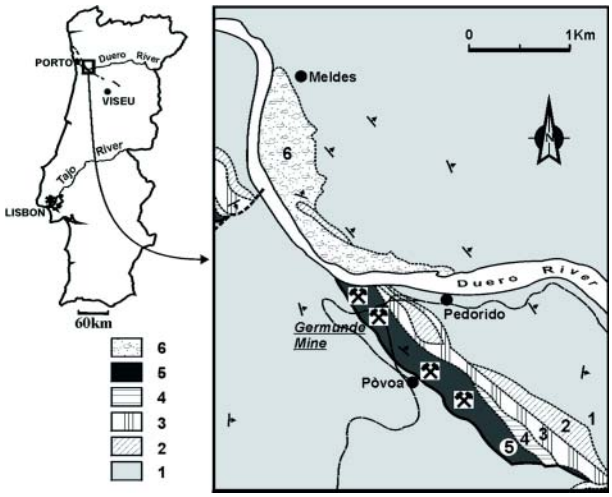

FIGURE 1. Geographical and geological location of the studied samples. (1) Xisto-Grauváquico Complex (Pre-Ordovician). (2) Armorican Quartzites. (3) Valongo Schists. (4) Schists and graywackes (2, 3, and 4 are Ordovician). (5) Stephanian C graywackes and shales. (6) Douro River alluvial deposits. (Adapted from 1/50.000 Portuguese Geological Map.)

composition of the gases produced was determined by means of a coupled FT-IR spectrometer. The NH_4 content of the <2 μm fraction was determined using Nessler's reagent on HF-digested samples.

Carbon-coated polished thin sections were studied by back-scattered electron (BSE) imaging using a ZEISS DSM 950 scanning electron microscope (SEM) and a four-spectrometer CAMECA-CAMEBAX SX-50 automated electron microprobe (EMP) at the C.I.C. and a JEOL 5800HV scanning electron microscope (SEM) at the University of Jaén. Minerals were recognized and chemically analyzed in the SEM using an X-ray energy dispersive (EDX) system (LINK QX 2000) at an accelerating voltage of 15 Kv and 2 nA beam current, using a 200 nm spot size and 100 s of live time. Operating conditions for the EMP were: acceleration voltage 20 kV; probe current 5 nA; electron beam diameter 0.5 μm. Albite (Na), orthoclase (K), periclase (Mg), wollastonite (Si and Ca), and synthetic oxides (Al_2O_3, Fe_2O_3, and $MnTiO_3$) were employed as standards and ZAF corrections were applied.

Samples for TEM analysis were selected from uncovered thin sections using a petrographic microscope. Copper grids with a single central hole 1 mm in diameter were glued to the sections, removed, and then thinned by an Ar ion mill (Gatan Dual Ion Milling 600 at C.I.C.). Two ion-milling conditions were used: (1) 6 kV, 1A, and 15° incident angle while perforating; and (2) 6 kV, low-angle (12°) and low-current (0.4A) final milling for ≈1 h to clean the sample surface. Samples were analyzed with a Philips CM20 scanning transmission electron microscope equipped with an EDAX solid-state EDX detector, operating at 200 kV, with a LaB_6 filament, and a point-to-point resolution of 2.7 Å (C.I.C., Granada University). Diffraction patterns were obtained from selected areas (SAED), and lattice-fringe images (HRTEM) were obtained following the procedures suggested by Buseck et al. (1988) and Buseck (1992). Areas for phyllosilicate analysis were carefully selected on lattice-fringe images to control the textural position and verify the absence of contamination by other phases. Quantitative analyses (AEM) were obtained only from thin edges, using a 50 Å beam diameter and a 1000 × 200 Å scanning area, with the long axis oriented parallel to the phyllosilicate packets. The samples were tilted 20° toward the detector. Albite, biotite, spessartine, muscovite, olivine, titanite, MnS, and CaS were used to obtain K-factors for the transformation of intensity ratios to concentration ratios following the procedures of Cliff and Lorimer (1975) and Champness et al. (1981). Loss of alkalis, especially K, is a significant problem in the analysis of defect-rich minerals (Van der Pluijm et al. 1988), and so shorter counting times (30 s) were used as a compromise for K analyses (Nieto et al. 1996).

AEM analyses were also obtained from powdered portions prepared using C-coated Cu grids. In this kind of preparation, thin individual grains of minerals are dispersed onto the grid with the (001) layers parallel to the sample surface. The monomineralic character of each grain analyzed was checked by electron diffraction. The data thus obtained are complementary to those taken from ion-milled samples as their orientation allows the use of a larger scanning window for analysis (1 μm × 1 μm), which provides better reproducibility of data and less loss of alkalis. The drawback is that textural information is lost.

RESULTS

X-ray diffraction

Samples Ge-6, Ge-7, and Ge-8 contain quartz, mica, and berthierine, which was identified from its 7.05 Å basal spacing and absence of changes with organic treatments. Figure 2 shows a representative XRD diagram of the samples. For higher 2θ angles, the (00*l*) peaks of micas become more and more divided between those corresponding to ≈10 Å (K-mica) and those to ≈10.15 Å (NH_4-mica). This splitting is obvious from the (003) peak for the <2 μm fraction and from the (002) peak for the 2–20 μm fraction. Unsplit low-angle peaks correspond to a $d_{001} \approx$ 10.15 Å and show some degree of asymmetry. The 10.15 Å series is more intense with respect to the 10 Å one for the <2 μm fraction than for the 2–20 μm fraction. The intensity relationships among the different orders of the same spacing are different for each kind of mica. They vary from those described by Juster et al. (1987) for both types of micas due to the effect of the automatic divergence slit. In our diffractometer, the normal I_{001}:I_{003} relationship for K-micas is 1:3 whereas the 10.15 Å series of the samples studied shows a 1:1 relationship. Organic treatments and heating to 550 °C do not produce any significant changes in the diffraction pattern, with the exception of the disappearance of the berthierine peaks after heating.

Table 1 presents the XRD parameters of the samples. Basal spacings in the range 10.12–10.18 Å are consistent with an NH_4-mica and the **b** parameters correspond to very low phengitic substitution. Because IC may be affected to some degree by the coexistence of two micas with slightly different d_{001}, their assignment to anchizone may be uncertain. Table 1

also shows the NH_4 contents obtained by the application of the criteria of Juster et al. (1987), Sucha et al. (1994), Drits et al. (1997), and Higashi (2000) to the basal spacings of the micas studied, which yield values ranging from 30 to 59% in the interlayer. No significant differences between the whole-rock, 2–20 μm, and <2 μm fractions have been observed either for d_{001} or for the intensity relationships.

To determine whether a part or all of the NH_4 was only weakly linked to the mica structure, samples were saturated with Mg. No change was detected either in the spacings or in the lack of response to organic treatments. For comparative purposes, Cabo de Gata smectite was saturated with NH_4. This treatment changed the basal spacing of smectite from 15.4 to 12.5 Å. Smectite maintained its swelling character, giving a spacing of 14.62 Å with ethylene glycol for the NH_4-treated sample and 17 Å for the untreated sample. Important changes in the relative intensities also could be detected after the NH_4 treatment in both the air-dried and EG smectites. Hence, it is concluded that the NH_4 belongs intrinsically to the mica structure.

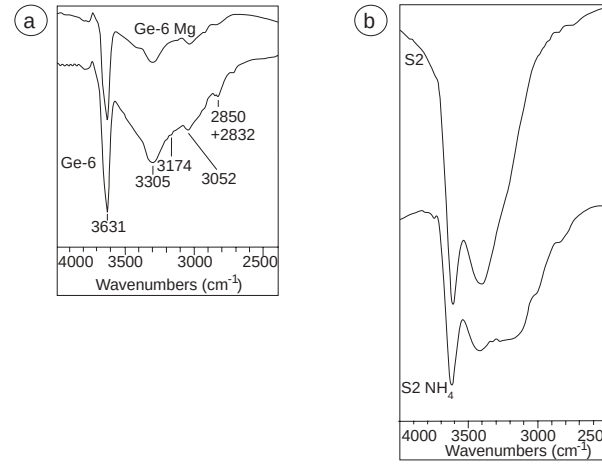

FIGURE 3. IR spectra of sample Ge-6 (**a**) and Cabo de Gata smectite (**b**). Ge-6 Mg is an Mg-saturated Germunde Mine sample and S2 NH_4 is an NH_4–saturated Cabo de Gata smectite.

Infrared spectrometry

A characteristic absorption band at 1430 cm^{-1} is evident in the IR spectra. This band does not change when the sample is Mg saturated. Different characteristic bands in the 3000–3400 cm^{-1} region, also unaffected by Mg saturation, are also present (Fig. 3a). These bands are absent in the spectrum of Cabo de Gata smectite, but were plainly evident when smectite was saturated with NH_4 (Fig. 3b). NH_4 saturated smectite also showed a band at 1400 cm^{-1}. Therefore, NH_4 is present in the mica structure and, in contrast to smectite, is firmly bonded, in the same way as the usual interlayer cations of mica.

TABLE 1. X-ray diffraction parameters

Samples	IC*	**b**	d_{001}	NH_4 content (% in interlayer)			
	(°2θ)	(Å)	(Å)	(1)	(2)	(3)	(4)
Ge-6	0.38	8.997	10.173	45	56	54	48
Ge-7	0.41	9.003	10.183	48	59	57	51
Ge-8	0.47	8.995	10.119	30	40	38	32

Notes: 1 = Juster et al. (1987); 2 = Sucha et al. (1994); 3 = Drits et al. (1997); 4 = Higashi (2000).
* IC converted to CIS.

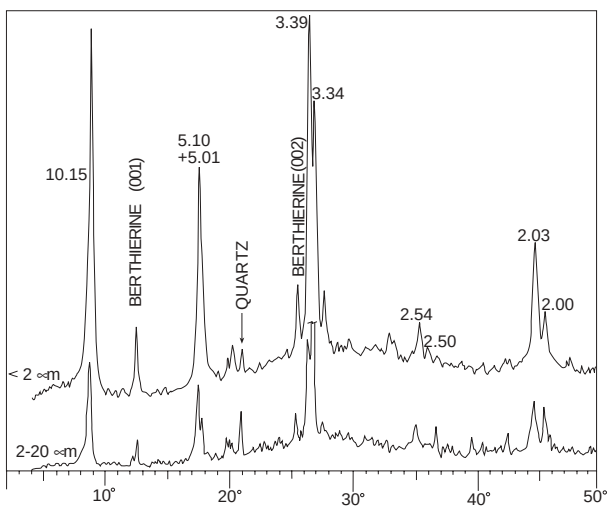

FIGURE 2. XRD patterns of the <2 μm and 2–20 μm fractions of sample Ge-6. Spacings in Å for the (00*l*) mica peaks are indicated.

Thermogravimetric analyses

Samples from the Germunde Mine show small, variable losses around 110 °C, corresponding to water. The most significant weight loss occurs between 300 and 650 °C with two main maxima: (1) between 544 °C (sample Ge-6) and 575 °C (sample Ge-7), which was identified as water; and (2) between 596 °C (sample Ge-7) and 610 °C (sample Ge-8), producing traces corresponding to CO_2. The overall loss, which cannot be split between the two maxima, is around 8.2 wt% for each of the three samples. Traces of CO and NO have been detected. The former at the same temperature as CO_2 and the latter between 620 and 640 °C. NH_3 has been detected only in trace amounts for sample Ge-7 at the same temperature as water and at 510 °C for sample Ge-8. It is concluded that NH_4 is not easily released from the mica structure by heating and the trace amounts of NH_3 are probably produced by the abundant organic matter present in the samples (as demonstrated by the release of CO_2 and CO).

Chemical analyses

Whole-rock compositions including the REE (Table 2[1]) are close to that of the PAAS (Post-Archean average Australian Shale, Taylor and McLennan 1985). The only notable anomaly is related with organic matter (a U enrichment over three times

[1]For a copy of Table 2, Document AM-01-003, contact the Business Office of the Mineralogical Society of America (see inside front cover of recent issue) for price information. Deposit items may also be available on the American Mineralogist web site at http://www.minsocam.org or current web address.

that of the PAAS).

Determination of NH_3 in the <2 μm fraction by means of Nessler's reagent produced the following results (in wt%): Ge-6 = 0.75, Ge-7 = 0.4, and Ge-8 = 0.95, with a margin of error = ±0.1.

Scanning electron microscopy and electron microprobe

Most of the fine intergrowths among quartz, berthierine, and NH_4- and K-micas are below the spatial resolution of BSE images and are therefore poorly resolved (Fig. 4). Likewise, NH_4-rich areas are too small to be analyzed properly either by SEM or EMP. Nevertheless, analysis of certain especially wide areas of the darker parts of micas in BSE images may correspond to tobelites (Table 3) and correlate well with those obtained with AEM (see below). Many analyses (not included in Table 3) show a Si content higher than 4. Therefore, selection of the darker areas of micas, in order to choose NH_4-rich zones in preference to K-rich ones, probably produced the inclusion of quartz-contaminated areas. As a consequence, many of the analyses included in Table 3 present overly high Si contents and, perhaps, unrealistically low K contents. Also, some of the analyses might represent intergrowths of NH_4-rich and K-rich micas. The lowest Si contents in the analyses are about 3.3 atoms per formula unit (afu), which correlates fairly well with Fe + Mg between 0.1 and 0.2, considering a small hypothetical illitic substitution (around 0.1) and an Fe^{3+} content that would presumably be low in this type of rocks (Guidotti and Sassi 1998b). For these analyses, K is around 0.4–0.5 afu Nitrogen has been detected qualitatively both in SEM and in EMP analyses, but the corresponding peak is too small to allow quantification.

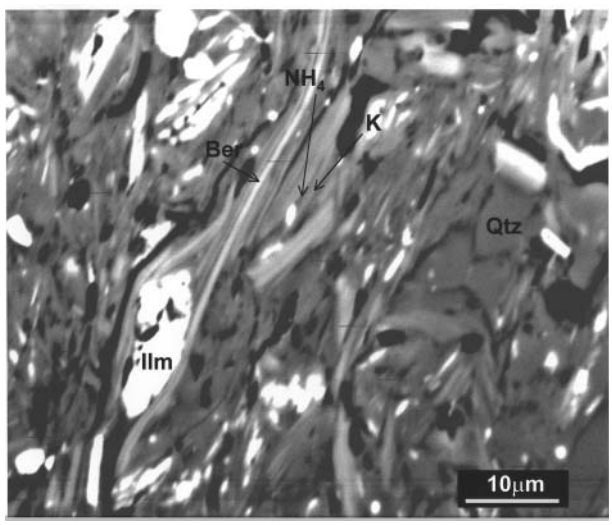

FIGURE 4. BSE image of a polished thin section of sample Ge-6. Ber = Berthierine, Ilm = Ilmenite, K = K-mica, NH_4 = NH_4-mica, Qtz = Quartz.

Transmission electron microscopy

Figure 5a is a representative low-magnification image of the general texture of the samples studied. The areas formed by phyllosilicates are composed of an intergrowth of sub-parallel packets of NH_4-mica, K-mica, and berthierine. The different packets, ranging in size from 100 to 500 Å, are separated from other packets of the same or a different phyllosilicate by low-angle boundaries. This range of sizes is typical of the anchizone (e.g., Merriman et al. 1990; Nieto and Sanchez Navas 1994; Arkai et al. 1996; Dalla Torre et al. 1996; Warr and Nieto 1998). Figure 5b is an enlarged view of an area from Figure 5a (arrow) showing the relationship between different packets of NH_4-mica and berthierine. Berthierine generally forms ≈100 Å packets with small tilts in relation to micas that usually prevent the proper orientation simultaneously for high resolution of both phyllosilicates.

Areas comprising various packets of only one kind of phyllosilicate are common (Fig. 6), which allows contamination-free AEM analyses. In a few cases, zones of ≈1 μm may be found. The general texture resembles those commonly described for very low-grade metamorphic pelites (Merriman and Peacor 1999). Each packet is composed of layers with constant spacing, and crystalline defects are not common. Curvature, such as commonly described for smectite or smectite-derived materials, is not present.

Fine intergrowths of NH_4- and K-micas are present but are not very abundant. Figure 7 shows packets of both micas that were identified by AEM. Analysis Ge-7a12 in Table 4 corresponds to the packet marked K, and analyses Ge-7a9 and Ge-7a10 to the area marked NH_4. Where the two micas are found together, K-mica may be distinguished by its darker contrast. Furthermore, NH_4-mica deteriorates very quickly and, in photographs taken after only a few tens of seconds, is easily recognized by the ubiquitous presence of alteration marks (see Fig. 5a). Layer partings such as those described for paragonite (Shau et al. 1991) are sometimes present in some cases.

SAED patterns of NH_4-micas show 00*l* diffraction spots with the three first orders in the same range of magnitude, in contrast to those generally found in K-micas in which the third one is clearly more intense (e.g., Nieto et al. 1996). The occurrence in the SAED of packets showing different orientations

TABLE 3. Chemical composition of tobelites determined by SEM and EMPA

	Si	^{IV}Al	^{VI}Al	Fe	Mg	Mn	Ti	K	Na	Ca	Σ int.
Ge-7-2	3.49	0.51	1.83	0.06	0.09	0.00	0.02	0.32	0.06	0.00	0.38
Ge-7-5	3.38	0.62	1.87	0.08	0.05	0.00	0.00	0.40	0.00	0.00	0.40
Ge-7-6	3.47	0.53	1.75	0.11	0.09	0.00	0.04	0.36	0.00	0.00	0.36
Ge-7-8	3.44	0.56	1.86	0.07	0.05	0.00	0.02	0.36	0.00	0.00	0.36
Ge-7-9	3.72	0.28	1.86	0.05	0.04	0.00	0.06	0.39	0.00	0.00	0.39
Ge-6-2*	3.31	0.69	1.82	0.04	0.07	0.00	0.07	0.47	0.05	0.01	0.53
Ge-6-3*	3.69	0.31	1.84	0.04	0.07	0.00	0.05	0.35	0.03	0.01	0.39
Ge-6-4*	3.27	0.73	1.79	0.07	0.13	0.00	0.01	0.53	0.04	0.01	0.59

Note: Each formula is normalized to six cations in tetrahedral and octahedral sites.
* EMPA data.

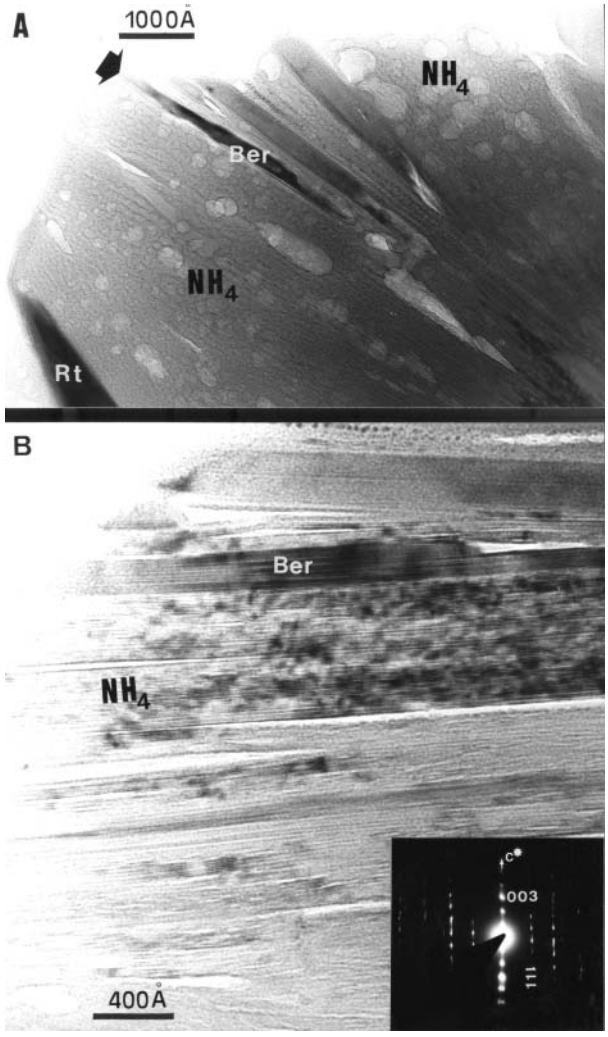

◀ **FIGURE 5.** (**A**) Low-magnification TEM image showing the general texture of a phyllosilicate-rich area in sample Ge-6. Note that areas of NH_4-micas are characteristically damaged after only a few seconds of observation. (**B**) Lattice-fringe image of area indicated by an arrow in Figure 5a. SAED pattern (inset) corresponds to a one-layer polytype. Rt = Rutile; NH_4 = Tobelite; Ber = Berthierine.

around c* (inset, Fig. 6) is common. Both one-layer (inset, Fig. 5b) and two-layer (inset, Fig. 6) polytypes are found. Although some disorder is always present, a predominant 10 or 20 Å periodicity may be recognized in all cases, and therefore, the 1Md polytype is not present. No relationship between polytype and chemical composition (determined by AEM) has been found. In some favorable cases, splitting of the third- or fourth-order 00*l* diffraction spots with a coherent difference between 10 and 10.15 Å can be recognized (inset, Fig. 8).

The existence of a tobelite–K-illite mixed-layer phyllosilicate was proposed by Juster et al. (1987) and studied using XRD methods by Drits et al. (1997). Therefore, the possible presence of similar mixed-layer phyllosilicates in our samples has been carefully checked. Only in sample Ge-7 have we distinguished an area showing periodic differences of contrast between layers (Fig. 8). An intermediate (00*l*) spot between the first and the second one (inset Fig. 8) may represent the superorder reflection of this mixed layer or dynamic diffraction effects of a two-layer polytype. Nevertheless, intermediate spots with similar intensity between the higher order reflections are also usually observed when the later possibility is right.

In conclusion, TEM images of these samples show all the usual characteristics of sub-greenschist samples. They are composed of small subparallel packets of a few layers of the different phyllosilicates coexisting in the sample. These packets change the orientation of the c* axis only slightly, but are each rotated around c*. Polytypes with different stacking order co-

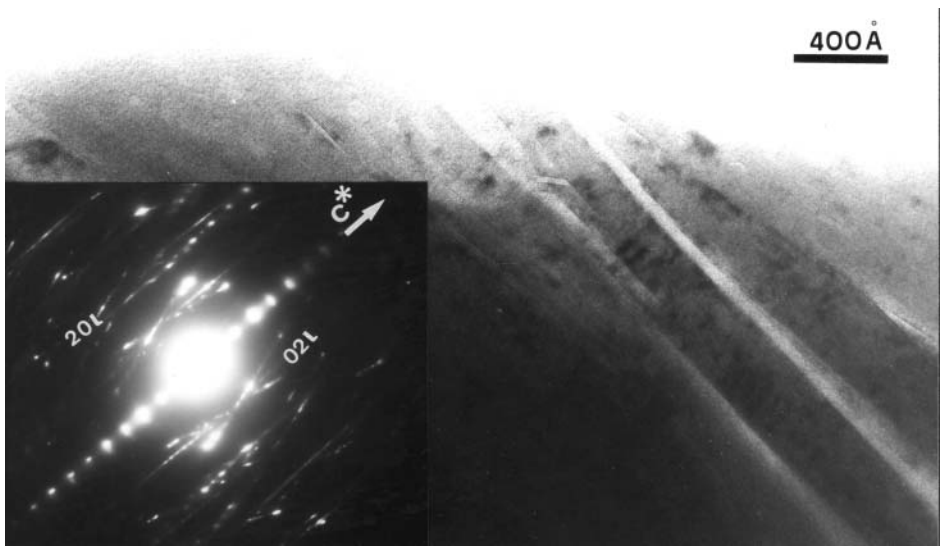

FIGURE 6. Lattice-fringe image of an area made up of subparallel packets of NH_4-mica (sample Ge-7). SAED pattern (inset) shows the coexistence of a*c* and b*c* orientations of 2-layer polytypes.

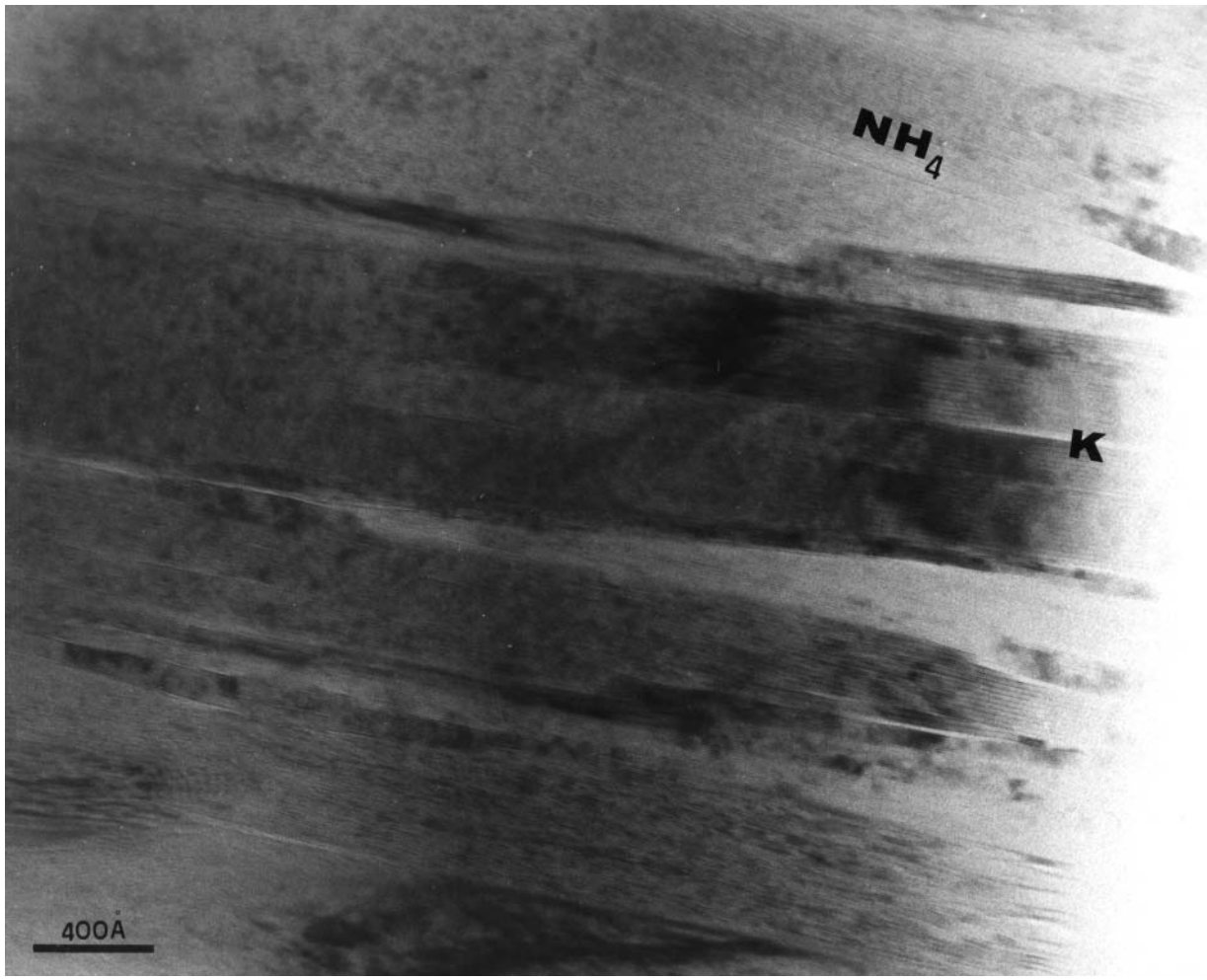

FIGURE 7. Intergrowth of tobelite (NH_4) and muscovite (K) in sample Ge-7. Area marked K includes analysis Ge-7a12 and the one marked NH_4 includes analyses Ge-7a9 and Ge-7a10 (see Table 4).

exist in the samples, and no systematic chemical differences are found between them, even with the chemical composition of each phase being far from homogeneous (see next section). All these characteristics imply the usual lack of equilibrium commonly described for sub-greenschist-facies samples (e.g., Merriman and Peacor 1999).

Analytical electron microscopy (AEM)

Table 4 shows the formulae of micas obtained by AEM. Both on ion-milled samples and powdered portions, a significant scattering of chemical compositions is present. This is in part a consequence of analytical problems, but also represents a true lack of chemical homogeneity, as is very common in very low-grade metapelites (Merriman and Peacor 1999). Nevertheless, some significant chemical tendencies may be recognized, in particular in the powdered samples, which are less affected by analytical problems such as K loss. Fe ranges from 0.01 to 0.16, but in most cases is lower than 0.1. Magnesium ranges from 0.04 to 0.21 in the powdered samples, with the most of the values between 0.1 and 0.15. Silicon presents some anomalously high figures in the analyses carried out on ion-milled samples, but the overall range of variation is reduced to 2.99–3.27 if only the analyzes of powdered sample are taken into account. Manganese is always lower than 0.01 and Ca has been detected only in one analysis of ion-milled sample Ge-7.

In agreement with XRD data and lattice-fringe images, two populations of micas can be clearly differentiated, based on the interlayer composition (Fig. 9). Great variation in the K + Na content is evident, partly due to cation loss, but no values have been found between 0.47 and 0.58. This compositional gap corresponds to 0.47–0.55 if only K is taken into account. In the low-K analyses, N has been detected qualitatively, but the corresponding peak in the EDX spectrum is too small to permit quantification, the same as in SEM and EMPA. The presence of N in the micas was also confirmed by electron energy loss spectroscopy (EELS) of powdered portions dispersed on holey-carbon grids (Livi et al. 2001).

Figure 10 shows the positive correlation between Si and Fe + Mg in NH_4- and K-micas. Titanium is present in minor amounts in the K-rich analyses, but is absent in the NH_4-micas.

TABLE 4. Composition of micas determined by AEM

	Si	^{IV}Al	^{VI}Al	Fe	Mg	Ti	K	Na
Ge-6m1	3.12	0.88	1.84	0.04	0.12	0.00	0.40	0.00
Ge-6m2	3.14	0.86	1.89	0.03	0.08	0.00	0.32	0.00
Ge-6m3	3.15	0.85	1.81	0.07	0.12	0.00	0.39	0.00
Ge-6m4	3.15	0.85	1.84	0.04	0.11	0.00	0.39	0.21
Ge-6m5	3.20	0.80	1.84	0.06	0.10	0.00	0.24	0.00
Ge-6m6	3.10	0.90	1.87	0.04	0.09	0.00	0.32	0.10
Ge-6m7	3.24	0.76	1.76	0.08	0.16	0.00	0.45	0.00
Ge-6m8	3.09	0.91	1.82	0.06	0.11	0.00	0.32	0.00
Ge-6m9	3.09	0.91	1.88	0.04	0.08	0.00	0.31	0.00
Ge-6m10	3.20	0.80	1.77	0.08	0.15	0.00	0.34	0.29
Ge-6m12	3.27	0.73	1.72	0.12	0.16	0.00	0.29	0.15
Ge-6m13	3.03	0.97	1.84	0.05	0.11	0.00	0.42	0.24
Ge-6m14	3.06	0.94	1.80	0.07	0.14	0.00	0.55	0.25
Ge-6m15	3.04	0.96	1.81	0.04	0.15	0.00	0.34	0.25
Ge-6m16	3.04	0.96	1.91	0.06	0.04	0.00	0.26	0.00
Ge-6m18	3.01	0.99	1.82	0.07	0.11	0.00	0.41	0.00
Ge-6m19	2.99	1.01	1.86	0.04	0.10	0.00	0.32	0.00
Ge-6m20	2.99	1.01	1.77	0.08	0.15	0.00	0.36	0.00
Ge-6m21	3.14	0.86	1.88	0.02	0.10	0.00	0.20	0.39
Ge-6m22	3.22	0.78	1.76	0.10	0.14	0.00	0.32	0.07
Ge-6m23	3.08	0.92	1.79	0.06	0.15	0.00	0.19	0.00
Ge-6m24	3.22	0.78	1.78	0.07	0.16	0.00	0.45	0.00
Ge-7m1	3.00	1.00	1.80	0.05	0.11	0.04	0.76	0.00
Ge-7m2	3.17	0.83	1.85	0.05	0.10	0.00	0.28	0.00
Ge-7m3	3.04	0.96	1.79	0.10	0.11	0.00	0.59	0.00
Ge-7m4	3.17	0.83	1.83	0.04	0.13	0.00	0.23	0.00
Ge-7m5	3.05	0.95	1.81	0.05	0.13	0.00	0.60	0.00
Ge-7m6	3.13	0.87	1.75	0.08	0.17	0.00	0.47	0.00
Ge-7m7	3.21	0.79	1.74	0.05	0.21	0.00	0.70	0.00
Ge-7m8	3.01	0.99	1.77	0.07	0.10	0.05	0.81	0.00
Ge-7m9	3.06	0.94	1.86	0.04	0.10	0.00	0.30	0.00
Ge-7m11	3.00	1.00	1.81	0.05	0.13	0.01	0.79	0.00
Ge-7m13	3.00	1.00	1.78	0.08	0.12	0.02	0.68	0.00
Ge-8m1	3.15	0.85	1.78	0.09	0.13	0.00	0.31	0.00
Ge-8m2	3.11	0.89	1.89	0.03	0.08	0.00	0.35	0.00
Ge-8m3	3.15	0.85	1.78	0.05	0.17	0.00	0.39	0.00
Ge-8m4	3.04	0.96	1.88	0.03	0.10	0.00	0.42	0.00
Ge-8m5	3.16	0.84	1.85	0.03	0.13	0.00	0.43	0.00
Ge-8m6	3.14	0.86	1.88	0.02	0.10	0.00	0.46	0.00
Ge-8m7	3.26	0.74	1.76	0.09	0.14	0.00	0.46	0.00
Ge-8m8	3.12	0.88	1.83	0.06	0.11	0.00	0.42	0.00
Ge-8m9	3.13	0.87	1.71	0.09	0.17	0.03	0.76	0.00
Ge-8m10	3.01	0.99	1.66	0.16	0.15	0.03	0.79	0.00
Ge-8m11	3.16	0.84	1.76	0.12	0.12	0.00	0.61	0.00
Ge-8m13	3.07	0.93	1.81	0.07	0.13	0.00	0.80	0.00
Ge-8m14	3.11	0.89	1.90	0.02	0.08	0.00	0.42	0.00
Ge-8m15	3.21	0.79	1.68	0.13	0.19	0.00	0.70	0.00
				Ion milling samples				
Ge-6a1	3.13	0.87	1.59	0.10	0.28	0.03	0.71	0.00
Ge-6a2	3.05	0.95	1.85	0.03	0.12	0.01	0.32	0.12
Ge-6a3	3.15	0.85	1.80	0.06	0.14	0.00	0.17	0.00
Ge-6a4	3.18	0.82	1.85	0.02	0.13	0.00	0.10	0.00
Ge-6a5	3.06	0.94	1.87	0.02	0.11	0.00	0.10	0.00
Ge-6a6	3.49	0.51	1.88	0.02	0.10	0.00	0.05	0.00
Ge-6a7	3.46	0.54	1.82	0.05	0.13	0.00	0.19	0.10
Ge-7a1	3.13	0.87	1.71	0.01	0.28	0.00	0.11	0.24
Ge-7a2	3.13	0.87	1.78	0.01	0.21	0.00	0.15	0.14
Ge-7a4	3.11	0.89	1.66	0.08	0.26	0.00	0.29	0.16
Ge-7a5	3.01	0.99	1.74	0.02	0.24	0.00	0.32	0.16
Ge-7a6	3.14	0.86	1.78	0.04	0.18	0.00	0.14	0.16
Ge-7a7	3.31	0.69	1.64	0.01	0.35	0.00	0.16	0.00
Ge-7a8	3.21	0.79	1.80	0.02	0.18	0.00	0.24	0.00
Ge-7a9	3.55	0.45	1.79	0.03	0.18	0.00	0.10	0.15
Ge-7a10	3.65	0.35	1.92	0.01	0.07	0.00	0.16	0.00
Ge-7a12	3.06	0.94	1.62	0.16	0.22	0.00	0.58	0.00
Ge-7a13	3.52	0.48	1.80	0.02	0.19	0.00	0.12	0.27
Ge-7a14	3.00	1.00	1.79	0.03	0.18	0.00	0.22	0.15
Ge-7a15	3.11	0.89	1.78	0.02	0.19	0.00	0.22	0.04

Note: Normalized to 6 cations in tetrahedral and octahedral sites.

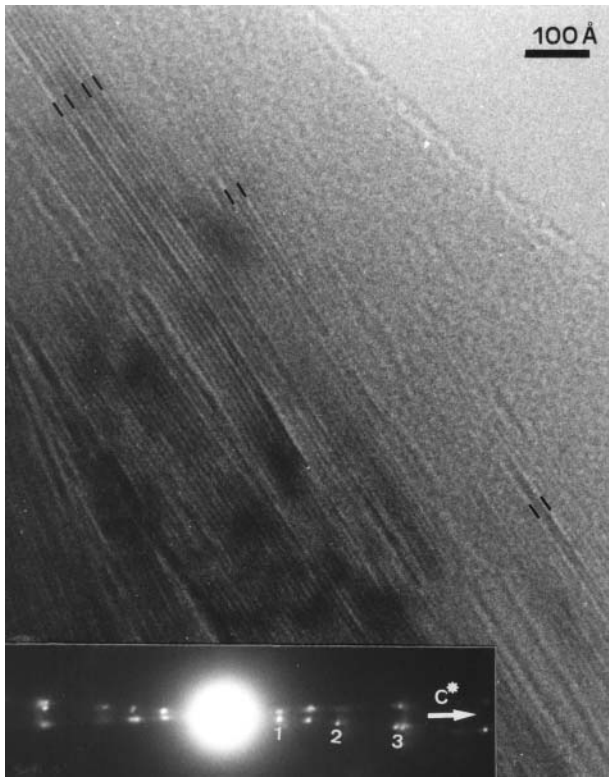

FIGURE 8. Tobelite/muscovite area including mixed-layers in sample Ge-7. Two- and three-layer periodicities are pointed out in the image. SAED pattern (inset) shows an intermediate (00*l*) spot between the first and the second one. Similar intermediate spots between higher-order reflections are absent. Splitting of the third (00*l*) spot between the spots corresponding to tobelite and muscovite can also be recognized.

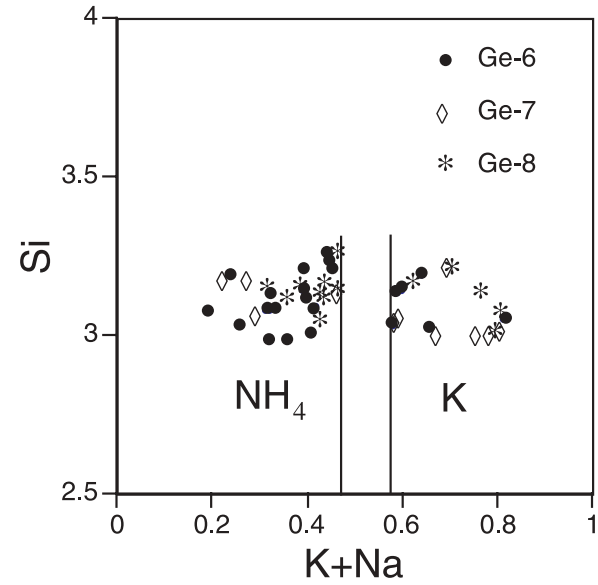

FIGURE 9. A plot of K + Na vs. Si (afu, based on 10 O atoms) of the powdered sample analyses of micas.

DISCUSSION

Physical nature of tobelites

The existence of an NH_4-mica in the Carboniferous shales of the *Bacia Carbonífera do Douro-Beira* has been demonstrated in accordance with all the criteria suggested by Juster et al. (1987), and in addition by electron microscopy observations and analyses. Some of the analyses, in particular those obtained by SEM and EMP, might seem to suggest a smectitic composition, due to the high Si content and the lack of exact information about interlayer population. One possibility to be considered is that a part of the NH_3 released in the decomposition experiments actually represents molecular NH_3 instead of bonded ionic NH_4. However, ionic exchange experiments have shown that when these samples are saturated with Mg, they do not change behavior either in XRD or in IR (Fig. 3). Exactly the opposite is true when smectite is saturated with NH_4. Moreover, TG indicates that only trace amounts of NH_3 are released below 900 °C. These trace amounts very likely arise from the organic matter contained in the samples, which in fact produce a significant amount of CO_2. Therefore, all the NH_4 contained in the phyllosilicate lattice appears to be truly bonded ionic NH_4. The high-Si content found, particularly in SEM and EMP analyses and in some AEM analyses of ion-milled samples, is most likely a consequence of analytical problems such as contamination by quartz.

Genetic conditions

Criteria for the establishment of metamorphic grade in subgreenschist-facies are generally very poor. In the *Bacia Carbonífera do Douro-Beira* shales, several different indicators have been used. Coal rank indicates a temperature of around 300 °C (Lemos de Sousa 1978). This temperature is consistent with the presence of pyrophyllite and paragonite in other samples and with the IC measurements.

The *Douro-Beira* NH_4 micas are associated with local coal seams, and have similar textural characteristics and mineral paragenesis as other widely described tobelites (Juster et al. 1987; Daniels and Altaner 1990; Wilson et al. 1992; Ward and Christie 1994; Sucha et al. 1994; Liu et al. 1996), although slightly higher in metamorphic grade. Their only significant chemical difference with normal shales is their organic-matter content. Therefore, it can be assumed that these samples formed by the generally accepted process in which NH_4 comes from the thermal maturation of organic matter and subsequent migration of N_2 contained in interlayered coal seams or in the pelitic rock itself.

Chemical characteristics of coexisting NH_4 and K-micas

The composition for both NH_4- and K-micas varies greatly from crystal to crystal, but lies within the usual range of dioctahedral micas for both tetrahedral and octahedral layers. The heterogeneity of chemical compositions of minerals formed during diagenesis and very low-grade metamorphism is a well-known fact (e.g., Li et al. 1994; Merriman et al. 1995; Dalla

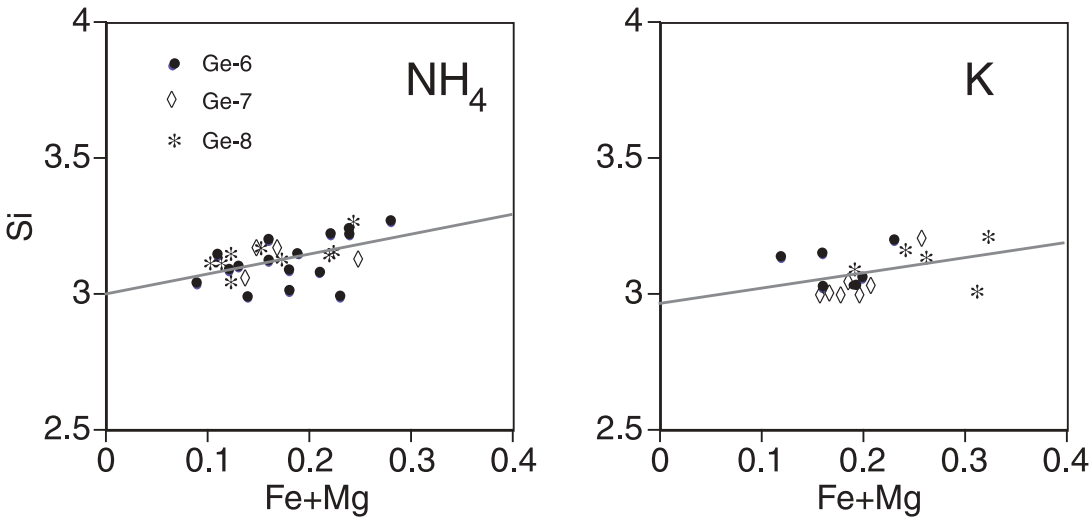

FIGURE 10. Plots of Si vs. Fe + Mg (afu, based on 10 O atoms) of both K-poor and K-rich mica populations (see Fig. 9).

Torre et al. 1996; Nieto et al. 1996; Livi et al. 1997; Giorgetti et al. 1997). The tschermak substitution affects NH_4- and K-micas similarly and produces a low amount of the phengite component in both types of micas (Fig. 10). This component agrees well with the **b** parameters determined from XRD (Table 1). No significant differences have been found between the NH_4- and K-micas. This is an interesting contrast to the Na-K system, in which paragonites show a distinctly lower phengite content than coexisting muscovites (e.g., Guidotti 1984). This contrasting behavior suggests that tobelite and muscovite are more alike than muscovite and paragonite regarding phengite content. The only detected chemical difference in the analyses presented in Table 4 is the low Ti content of K-micas as opposed to a complete lack of Ti in the NH_4-micas.

Because NH_4 cannot be directly quantified for such small grain sizes, indirect means must be used to quantify its occurrence in the samples. One indication may be the 1–(K + Na) difference in the interlayer site, but this fails to take into account a possible illitic substitution. A good approximation to the mean value of each sample may be obtained from the d_{001}, but this parameter gives a mean value at the sample level and does not allow the important differences among grains in the same sample to be monitored. The NH_4 content obtained from d_{001} varies according to the methods proposed by different authors (Table 1), probably due to the effect on d_{001} of other chemical variables, particularly phengite content (Guidotti 1992). According to these data, NH_4 may constitute 30–59% of the interlayer positions in the Douro-Beira tobelites, which is in good agreement with the K + Na content obtained in AEM (Fig. 9). Finally, the amount of NH_3 of the <2 μm fraction determined using Nessler's reagent is another indication of the mean value of each sample. The 0.4–0.5 afu of NH_4 would represent 1.8–2 wt% of the mica. Taking into account the measured NH_3 of the <2 μm fraction (0.75–0.95%), the results are consistent if the NH_4-mica represents 40–50% of the overall <2 μm fraction, which is a highly reasonable assumption (Fig. 2).

Chemical analyses of natural tobelites and NH_4-micas, determined by EMP methods, have been reported by Daniels and Altaner (1990, Table 3) and Wilson et al. (1992, Table 3). The latter include in-situ determination of the NH_4 content. Our results agree perfectly with those data, even though the genetic contexts of the three cases are different (coal fractures for the sample of Daniels and Altaner and hydrothermal veins for those of Wilson et al.).

Due to the lack of direct in-situ data about the NH_4 content, doubt remains regarding the existence of an illitic substitution in the Douro-Beira micas. The maximum determined K + Na content of the Douro-Beira samples is around 0.8 afu but, as with the NH_4-micas that contain K, the K micas most likely contain some NH_4, thus possibly filling the interlayer positions. Moreover, no obvious illitic substitution may be recognized in Figure 9. The excess of Si over 3 is perfectly compensated by Mg + Fe^{2+}, even if we accept the possibility of some Fe^{3+}. Therefore, no evidence of illitic substitution can be found in the Douro-Beira micas and they should be considered as muscovites or their NH_4 equivalent.

Miscibility gap between NH_4 and K-micas

Drits et al. (1997) found that illite layers formed during the diagenesis of North Sea oil source rocks were actually tobelite layers, and that illite-smectite have K end-member illite and NH_4 end-member illite layers. Similar behavior among smectite, illite, and tobelite layers was described by Lindgreen et al. (2000) in black Cambrian Alum shales from the Baltic area. In the very-low grade metamorphic rocks of Pennsylvania, Juster et al. (1987) found minor amounts of NH_4/K mixed-layers. Although the majority of the micas were discrete NH_4- or K-illites, mixed-layers were still recognized by XRD.

For the Douro-Beira samples, which, according to mineralogical and coal data, represent the highest temperature of the three cases, NH_4/K mixed-layers have been recognized only by TEM in one small area (Fig. 8) and are absolutely undetect-

able by XRD. It can be concluded that, in contrast to the lower-temperature cases of Pennsylvania (Juster et al. 1987) and the North Sea (Drits et al. 1997), the NH_4 and K areas are segregated into well-separated packets with only minor intergrowths and a nearly complete lack of interlayering. NH_4 and K coexist in the same layer, but one cation is dominant. Thus, the evolution of tobelite during low-grade metamorphism follows a path of metastable mixed compositions that increase in segregation as grade increases. This path is similar to the evolution of paragonite and margarite (Livi et al. 1997).

The existence of a compositional gap between the K- and NH_4-micas was proposed by Juster et al. (1987). In the Douro-Beira samples, the simultaneous presence of two groups of mica compositions, one K rich and the other K poor, is demonstrated by XRD diagrams (Fig. 2), lattice fringe images (Fig. 7), SAED (inset Fig. 8), and AEM data (Fig. 9). The textural relationship between the two micas is the usual one between paragenetic phyllosilicates in very low-grade shales (see the "Transmission electron microscopy" section for a complete description) and exactly like the one described for the muscovite-paragonite system (Shau et al. 1991). The compositional gap is narrow (Fig. 9), possibly near its closure. This closure, however, might not even occur due to the instability of NH_4-micas at higher temperatures.

ACKNOWLEDGMENTS

Thanks to B. Valle Agüado for the samples and geological information about them; M. Sanchez Viñas for the Nessler's reagent determination of NH_3; K. Livi for his useful correction of the first manuscript and EELS analysis; J. Cuadros for the Cabo de Gata smectite sample and useful comments; J. Lopez Garzon for his help in the interpretation of IR and TG results; J. Jiménez-Millán for his help with SEM; M. Mellini for useful discussion and ideas; D. Morata for his help in the interpretation of the chemical compositions of the rocks; and C. Laurin for polishing the English. The useful comments of C.V. Guidotti and J.C. Schumacher have greatly improved the quality of the paper. The help of the following technicians in their respective instruments or techniques has been fundamental for the present work: M.M. Abad-Ortega (HRTEM-AEM), A. Caballero (drawing), B. Funes (IR), I. Guerra (SEM), M.A. Hidalgo-Laguna (EMP), A. Molina-Illescas (photographic laboratory), J.D. Montes-Rueda (ion mill), I. Nieto (Preparation of samples), M.A. Salas (TG), P. Sanchez-Gómez (XRD). Financial support was supplied by Research Project no. BTE-2000-0582 of the Spanish Ministry of Education and Research Group RNM-0179 of the Junta de Andalucía.

REFERENCES CITED

Arkai, P., Merriman, R.J., Roberts, B., Peacor, D.R., and Tóth, M. (1996) Crystallinity, crystallite size and lattice strain of illite-muscovite and chlorite: comparison of XRD and TEM data of diagenetic to epizonal pelites. European Journal of Mineralogy, 8, 1119–1137.

Barrier, R.M. and Dicks, L.W.R. (1966) Chemistry of Soil Minerals. Part III. Synthetic micas with substitutions of NH_4 for K, Ga for Al, and Ge for Si. Journal of Chemical Society A, 1379–1385.

Bobos, I. and Ghergari, L. (1999) Coversion of smectite to ammonium illite in the hidrothermal system of Harghita Băi, Romania: SEM and TEM investigations. Geologica Carpathica, 50, 379–387.

Boyd, S.R. (1997) Determination of the ammonium content of potassic rocks and minerals by capacitance manometry - a prelude to the calibration of FTIR microscopes. Chemical Geology, 137, 57–66.

Buseck, P.R. (1992) Principles of transmission electron microscopy. In P.R. Buseck, Ed., Minerals and reactions at the atomic scale: transmission electron microscopy, 27, p. 1–35. Reviews in Mineralogy, Mineralogical Society of America, Washington, D.C.

Buseck, P.R., Cowley, J.M., and Eyring, L. (1988) High-resolution transmission electron microscopy and associated techniques, 128 p. Oxford University Press, New York.

Champness, P.E., Cliff, G., and Lorimer, G.W. (1981) Quantitative analytical electron microscopy. Bulletin de Minéralogie, 104, 236–240.

Cliff, G. and Lorimer, G.W. (1975) The quantitative analysis of thin specimens. Journal of Microscopy, 103, 203–207.

Cooper, J.E. and Abedin, K.Z. (1981) The relationship between fixed ammonium-nitrogen and potasium in clays from a deep well on the Texas Gulf Coast. Texas Journal of Science, 33, 103–111.

Cuadros, J. and Altaner, S.P. (1998) Characterization of mixed-layer illite-smectite from bentonites using microscopic, chemical, and X-ray methods: Constraints on the smectite-to-illite transformation mechanism. American Mineralogist, 83, 762–774.

Cuadros, J. and Linares, J. (1996) Experimental kinetic study of the smectite-to-illite transformation. Geochimica et Cosmochimica Acta, 60, 439–453.

Dalla-Torre, M., Livi, K., Veblen, D.R., and Frey, M. (1996) White K-mica evolution from phengite to muscovite in shales and shale matrix melange, Diablo Range, California. Contribution to Mineralogy and Petrology, 123, 390–405.

Daniels, E.J. and Altaner, S.P. (1990) Clay mineral authigenesis in coal and shale from the Anthracite region, Pennsylvania. American Mineralogist, 75, 825–839.

Drits, V.A., Lindgreen, H., and Salyn, A.L. (1997) Determination of the content and distribution of fixed ammonium in illite-smectite by X-ray diffraction: Application to North Sea illite-smectite. American Mineralogist, 82, 79–87.

Duit, W., Jansen, J.B.H., van Bremen, A., and Bos, A. (1986) Ammonium micas in metamorphic rocks as exemplified by Dome de l'Agout (France). American Journal of Science, 286, 702–732.

Eugster, H.P. and Muñoz, J. (1966) Ammonium micas: Possible sources of atmospheric ammonia and nitrogen. Science, 151, 683–686.

Frey, M. (1987) Very low-grade metamorphism of clastic sedimentary rocks. In M. Frey, Ed. Low temperature metamorphism, p. 9–58. Blackie, Glasgow.

Giorgetti, G., Memmi, I., and Nieto, F. (1997) Microstructures of intergrown phyllosilicate grains from Verrucano metasediments (Northern Apennines, Italy). Contributions to Mineralogy and Petrology, 128, 127–138.

Gromet, L.P., Dymek, R.F., Haskin, L.A., and Korotev, R.L. (1984) "The North American Shale Composite": its compilation, major an trace element characteristics. Geochimica et Cosmochimica Acta, 48, 2469–2482.

Guidotti, C.V. (1984) Micas in metamorphic rocks. In S.W. Bailey, Ed., Micas, 13, p. 357–467. Mineralogical Society of America, Washington, D.C.

Guidotti, C.V. and Sassi, F.P. (1998a) Miscellaneous isomorphous substitutions in Na-K white mica; a review, with special emphasis to metamorphic micas. Rendiconti Lincei Scienze Fisiche e Naturali, 9, 57–78.

———(1998b) Petrogenetic significance of Na-K white mica mineralogy: Recent advances for metamorphic rocks. European Journal of Mineralogy, 10, 815–854.

Guidotti, C.V., Mazzoli, C., Sassi, F.P., and Blencoe, J.G. (1992) Compositional controls on the cell dimensions of $2M_1$ muscovite and paragonite. European Journal of Mineralogy, 4, 283–297.

Hashizume, H., Yamada, H., and Nakazawa, H. (1995) Alteration of smectite in a system including alanine at high-pressure and temperature. Clays and Clay Minerals, 43, 184–190.

Higashi, S. (1982) Tobelite, a new ammonium dioctahedral mica. Mineralogical Journal, 11, 138–146.

———(2000) Ammonium-bearing mica and mica/smectite of several pottery stone and pyrophyllite deposits in Japan: their mineralogical properties and utilization. Applied Clay Science, 16, 171–184.

Jiang, W.T. and Peacor, D.R. (1993) Formation and modification of metastable intermediate sodium potasium mica, paragonite, and muscovite in hydrothermally altered metabasites from North Wales. American Mineralogist, 78, 782–793.

Juster, T.C., Brown, P.E., and Bailey, S.W. (1987) NH_4-bearing illite in very low grade metamorphic rocks associated with coal, northeastern Pennsylvania. American Mineralogist, 72, 555–565.

Kisch, H.J. (1991) Illite crystallinity: recommendations on sample preparation, X-ray diffraction settings, and interlaboratory samples. Journal of Metamorphic Geology, 9, 665–670.

Lemos de Sousa, M.J. (1978) O grau de incarbonizaçao (rang) dos carvões durienses e as consequencias genéticas, geológicas e estruturais que resultam do seu conhecimento. Comunicações dos Serviços Geologicos de Portugal, 63, 179–365.

Li, G.J., Peacor, D.R., Merriman, R.J., and Roberts, B. (1994) The diagenetic to low-grade metamorphic evolution of matrix white micas in the system muscovite-paragonite in a mudrock from Central Wales, United-Kingdom. Clays and Clay Minerals, 42, 369–381.

Lindgreen, H. (1994) Ammonium fixation during illite-smectite diagenesis in Upper Jurassic shale, North-Sea. Clay Minerals, 29, 527–537.

Lindgreen, H., Drits, V., Sakharov, B.A., Salyn, A.L., Wrang, P., and Dainyak, L.G. (2000) Illite-smectite structural changes during metamorphism in black Cambrian Alum shales from the Baltic area. American Mineralogist, 85, 1223–1238.

Liu, Q., Zhang, P., Ding, S., Lin, X., and Zheng, N. (1996) NH_4-illite in Permo-Carboniferous coal-bearing strata, North China. Chinese Science Bulletin, 41, 1458–1461.

Livi, K.J.T., Veblen, D.R., Ferry, J.M., and Frey, M. (1997) Evolution of 2:1 layered silicates in low-grade metamorphosed Liassic shales of Central Switzerland. Journal of Metamorphic Geology, 12, 323–344.

Livi, K.J.T., Abad, I., Veblen, D., and Nieto, F. (2001) EELS Analysis of Micas. EUG XI, p. 673, Estrasburgo.

Merriman, R.J. and Peacor, D.R. (1999) Very low-grade metapelites: mineralogy, microfabrics and measuring reaction progress. In M. Frey, and D. Robinson, Eds., Low-Grade Metamorphism, p. 10–60. Blackwell Science, Oxford.

Merriman, R.J., Roberts, B., and Peacor, D.R. (1990) A transmission electron microscope study of white mica crystallite size distribution in a mudstone to slate transitional sequence, North Wales, U.K. Contributions to Mineralogy and Petrology, 106, 27–40.

Merriman, R.J., Roberts, B., Peacor, D.R., and Hirons, S.R. (1995) Strain-related differences in the crystal growth of white mica and chlorite: a TEM and XRD study of the development of metapelitic microfabrics in the Southern Uplands thrust terrane, Scotland. Journal of Metamorphic Geology, 13, 559–576.

Nieto, F. and Sánchez-Navas, A. (1994) A comparative XRD and TEM study of the physical meaning of the white mica "crystallinity" index. European Journal of Mineralogy, 6, 611–621.

Nieto, F., Ortega-Huertas, M., Peacor, D., and Arostegui, J. (1996) Evolution of illite/smectite from early diagenesis through incipient metamorphism in sediments of the Basque-Cantabrian Basin. Clays and Clay Minerals, 44, 304–323.

Sassi, F.P. and Scolari, A. (1974) The b_o value of the potassium white micas as a barometric indicator in low-grade metamorphism of pelitic schits. Contributions to Mineralogy and Petrology, 45, 143–152.

Schroeder, P.A. and McLain, A.A. (1998) Illite-smectites and the influence of burial diagenesis on the geochemical cycling of nitrogen. Clay Minerals, 33, 539–546.

Shau, J.H., Feather, M.E., Essene, E.J., and Peacor, D.R. (1991) Genesis and solvus relations of submicroscopically intergrown paragonite and phengite in a blueschist from northern California. Contribution to Mineralogy and Petrology, 106, 367–378.

Shigorova, T.H., Kotov, N.V., Kotel´nikova, Y.N., Shamakin, B.M., and Frank-Kamenetskiy, V.A. (1981) Synthesis, diffractometry, and IR spectroscopy of micas in the series from muscovite to the ammonium analog. Geochemistry International, 18, 76–82.

Sucha, V., Kraus, I., and Madejova, J. (1994) Ammonium illite from anchimetamorphic shales associated with anthracite in the Zemplinicum of the Western Carpathians. Clay Minerals, 29, 369–377.

Sucha, V., Elsass, F., Eberl, D.D., Kuchta, L., Madejova, J., Gates, W.P., and Komadel, P. (1998) Hydrothermal synthesis of ammonium illite. American Mineralogist, 83, 58–67.

Taylor, S.R. and McLennan, S.M. (1985) The Continental Crust: Its composition and evolution. 321 p. Blackwell, Oxford.

Van Der Pluijm, B.A., Lee, J.H., and Peacor, D.R. (1988) Analytical electron microscopy and the problem of potassium diffusion. Clays and Clay Minerals, 36, 498–504.

Ward, C.R. and Christie, P.J. (1994) Clays and other minerals in coal seams of the Moura-Baralaba area, Bowen Basin, Australia. International Journal of Coal Geology, 25, 287–309.

Warr, L.N. and Nieto, F. (1998) Crystallite thickness and defect density of phyllosilicates in low temperature metamorphic pelites: a TEM and XRD study of clay-mineral crystallinity-index standards. Canadian Mineralogist, 36, 1453–1475.

Warr, L.N. and Rice, A.H.N. (1994) Interlaboratory standardization and calibration of clay mineral crystallinity and crystallite size data. Journal of Metamorphic Geology, 12, 141–152.

Williams, L.B. and Ferrell, R.E. (1991) Ammonium substitution in illite during maturation of organic-matter. Clays and Clay Minerals, 39, 400–408.

Williams, L.B., Ferrell, R.E., Chinn, E.W., and Sassen, R. (1989) Fixed-ammonium in clays associated with crude oils. Applied Geochemistry, 4, 605–616.

Williams, L.B., Wilcoxon, B.R., Ferrell, R.E., and Sassen, R. (1992) Diagenesis of ammonium during hydrocarbon maturation and migration. Applied Geochemistry, 7, 123–134.

Wilson, P.N., Parry, W.T., and Nash, W.P. (1992) Characterization of hydrothermal tobelitic veins from black shale, Oquirrh Mountains, Utah. Clays and Clay Minerals, 40, 405–420.

MANUSCRIPT RECEIVED FEBRUARY 26, 2001
MANUSCRIPT ACCEPTED OCTOBER 21, 2001
MANUSCRIPT HANDLED BY JOHN C. SCHUMACHER